

Possible involvement of both endoplasmic reticulum- and mitochondria-dependent pathways in MoMuLV-*ts1*-induced apoptosis in astrocytes

Na Liu,¹ Xianghong Kuang,¹ Hun-Taek Kim,² George Stoica,² Wenan Qiang,¹ Virginia Lee Scofield,¹ and Paul KY Wong¹

¹Department of Carcinogenesis, University of Texas, MD Anderson Cancer Center, Science Park-Research Division, Smithville, Texas, USA and ²Department of Pathology (HTK, GS), Texas A&M University, College Station, Texas, USA

The Moloney murine leukemia virus (MoMuLV)-*ts1* retrovirus, a naturally occurring mutant of MoMuLV-TB, causes a neuroimmunodegenerative syndrome in mice. The authors show here that *ts1* triggers apoptosis in immortalized astrocytes, C1 cells, and primary cultured astrocytes, and that this apoptosis is caused by endoplasmic reticulum (ER) stress resulting from accumulation of the viral envelope preprotein gPr80^{env}. In *ts1*-infected C1 cells, an unfolded protein response was identified by activation of the ER-resident transmembrane protein kinase PERK, an event that leads to hyperphosphorylation of eIF2 α , up-regulation of GRP78, increased amounts of GADD153/CHOP, and cleavage of procaspase-12. Up-regulation of GRP78 and cleavage of procaspase-12 were also detected in primary cultured astrocytes infected with *ts1*. In *ts1*-infected C1 cells, ER stress was followed by mitochondrial stress, detected as mitochondrial transmembrane potential dissipation, cleavage of procaspase-9, and induction of activated caspase-3. In the brain-stems of *ts1*-infected mice, activated caspase-3 and damaged mitochondria were identified in astrocytes within areas showing spongiform degeneration. Together the data imply that both ER stress- and mitochondrial stress-related apoptotic pathways are involved in *ts1*-induced astrocyte death. *Journal of NeuroVirology* (2004) 10, 189–198.

Keywords: apoptosis; astrocyte; caspase; ER stress; mitochondrial stress; MoMuLV-*ts1*

Introduction

The murine retrovirus *ts1*, a mutant of Moloney murine leukemia virus (MoMuLV), induces a progres-

sive neuroimmunodegenerative syndrome in mice that has many similarities to human acquired immunodeficiency syndrome (AIDS), and the *ts1* mouse has been used to model human immunodeficiency virus (HIV) disease (Gonzales-Scarano *et al*, 1995; Wong *et al*, 1998; Clark *et al*, 2001). Clinical manifestations of *ts1* infection include hindlimb paralysis, wasting, and immunodeficiency (Wong *et al*, 1998; Clark *et al*, 2001). Pathological changes in the central nervous system (CNS) of the *ts1* mouse include neuronal loss and gliosis, which are also present in the brains of humans with a variety of neurodegenerative diseases, such as HIV-associated dementia (Gonzales-Scarano *et al*, 1995), prion diseases (Diedrich *et al*, 1991), and amyotrophic lateral sclerosis (Mourelatos *et al*, 1994). In addition, the spongiform degeneration in the CNS of the *ts1* mouse, a type of lesion described only rarely in HIV encephalitis, represents the hallmark of an

Address correspondence to Paul K. Y. Wong, Department of Carcinogenesis, University of Texas, MD Anderson Cancer Center, Science Park-Research Division, Smithville, TX 78957, USA. E-mail: pwong@sprd1.mdacc.tmc.edu

The authors thank Vanessa Edwards for her assistance in preparing the manuscript, and Dr. Mingshan Yan and Jodi Cahill for their generous help. The authors are also most grateful to Dr. Kaoru Kiguchi of this Department and to Kent Claypool of the Cell and Tissue Analysis Facility Core in Science Park for their assistance. This work was supported by NIH grants AI28283, NS43984, NCI Cancer Center Support grant (CA16672), and NIEHS Center grant (ES07784).

Received 18 December 2003; revised 9 February 2004; accepted 13 February 2004.

unusual form of neurodegeneration caused by transmissible spongiform encephalopathy (TSE) agents or prions (Dimcheff *et al*, 2003). The molecular and cellular events associated with spongiform degeneration are not clear. However, a recent study of transcriptional profiles from mice infected with another murine neurovirulent retrovirus (FrCas^E) suggest that spongiform degeneration occurring in the context of retroviral CNS infection may be due to protein misfolding in the endoplasmic reticulum, or ER (Dimcheff *et al*, 2003).

In CNS tissues of *ts1*-infected mice, astrocytes, microglia, oligodendrocytes, and endothelial cells are infected with *ts1*, but neurons are not (Stoica *et al*, 1993). As neuron-supporting cells, astrocytes play a crucial role in the maintenance of normal neuronal function. Astrocyte dysfunction has been shown to contribute to neuronal death and degeneration (Atwood *et al*, 1993; Wong and Lynn, 1997; Brack-Werner, 1999; Friedlander, 2003; Galey *et al*, 2003). Notably, in prion disease, protein PrP^{Sc} accumulation in astrocytes occurs prior to astrogliosis, vacuolation, and neuronal loss (Diedrich *et al*, 1991), and the extent of neuronal loss is closely correlated with ER stress-related apoptosis (Hetz *et al*, 2003).

The envelope preprotein gPr80^{env} of the *ts1* virus is structurally different from that of the parent viral strain MoMuLV-TB, because of a point mutation in its encoding *env* sequence. In cultured murine astrocytes infected by *ts1*, the mutant gPr80^{env} is processed abnormally, resulting in the formation of aggregates in the ER (Szurek *et al*, 1990; Shikova *et al*, 1993; Lin *et al*, 1997). The simultaneous occurrence of gPr80^{env} accumulation and cell death has led us to propose that *ts1* infection causes an ER stress response in astrocytes (Liu *et al*, 2002).

In general, ER stress stimuli activate two distinct signal transduction pathways, which are the ER overload response, or EOR, and the unfolded protein response, or UPR (Kozutsumi *et al*, 1988; Pahl and Baeuerle, 1996). The EOR causes nuclear factor kappa B (NF κ B) activation and translocation to the nucleus by activating IKK (inhibitor of κ B kinase), allowing degradation of the inhibitor of NF κ B (I κ B). In the nucleus, NF κ B induces the expression of genes encoding proteins involved in inflammatory responses, such as tumor necrosis factor alpha (TNF α), Fas, and inducible nitric oxide synthase (iNOS) (Baeuerle and Baichwal, 1997; May and Ghosh, 1998). In the UPR, the ER transmembrane kinases IRE1 (inositol-requiring enzyme 1) and PERK (PKR-like ER kinase) are activated, and the two act together to up-regulate the expression of ER stress response genes. These include genes encoding chaperones such as GRP78 and GRP94, and the growth arrest and DNA damage gene, *gadd153*. In this context, chaperones serve to delay the onset of apoptosis by facilitating protein folding in ER, whereas GADD153 serves as a death signal. PERK activation also induces phosphorylation of the translation initiation factor eIF2 α , which

causes global inhibition of protein synthesis (Harding *et al*, 2000; Yoshida *et al*, 2000, 2001). Like chaperone protein production, this response facilitates protein folding in the ER, in this case, by allowing more time for protein transit through the ER to the Golgi compartment.

The ER can also convey stress information to mitochondria by a variety of signals (Hacki *et al*, 2000; Nakamura *et al*, 2000; Hori *et al*, 2002; Jacobson and Duchen, 2000). In response to these signals, mitochondrial membrane permeabilization occurs, resulting in release of cytochrome *c*, activation of the caspase-9-related apoptotic pathway, and loss of the mitochondrial transmembrane potential ($\Delta\Psi_m$), leading to overproduction of reactive oxygen species (ROS) and to redox imbalance in the cell (Kroemer and Reed, 2000).

In most cell types, apoptosis is mediated by activated caspases, which are synthesized as inactive proenzymes and activated by proteolytic cleavage. The particular caspases activated during an apoptosis event can identify the signaling pathway(s) that are involved in cell death. For example, the cleavage and activation of procaspase-12 is specifically linked to ER stress-induced apoptosis (Nakagawa *et al*, 2000; Rao *et al*, 2001). On the other hand, caspase-9 activation is the unique marker that identifies apoptosis caused by mitochondrial stress (Li *et al*, 1997). Activated caspase-3 acts as common downstream effector for both of these apoptotic cascades.

We show here that cultured astrocytes infected with *ts1* exhibit both the manifestations of ER stress (phosphorylation of eIF2 α , induction of GADD153/CHOP, up-regulation of the chaperone proteins GRP78 and GRP94, and procaspase-12 cleavage) and the markers for mitochondrial stress ($\Delta\Psi_m$ dissipation, procaspase-9 and procaspase-3 cleavage). These results support the idea that astrocyte death following *ts1* infection is due to ER and mitochondrial stress.

Results

ts1 induces apoptosis in infected astrocytes

Propidium iodide (PI) staining and flow cytometry are suitable for quantitative studies of apoptosis (sub-G1 peak) in astrocytes (Micoud *et al*, 2001). Figure 1 shows that the percentage of C1 cells in the sub-G1 peak at 72 h post infection (p.i.) was 51% for *ts1*-infected cells, relative to 2% for control uninfected cells ($P < .01$). Apoptosis apparently began before 48 h p.i., because the percentage of sub-G1 cells in *ts1*-infected cultures was increased 18-fold by 48 h p.i. ($P < .05$; data not shown).

To confirm that this result reflects apoptosis in *ts1*-infected C1 cells, we used Hoechst 33342 and PI together to stain infected and uninfected cells, followed by microscopic comparison of nuclear morphology in the two cell populations. In Figure 2, the nuclei

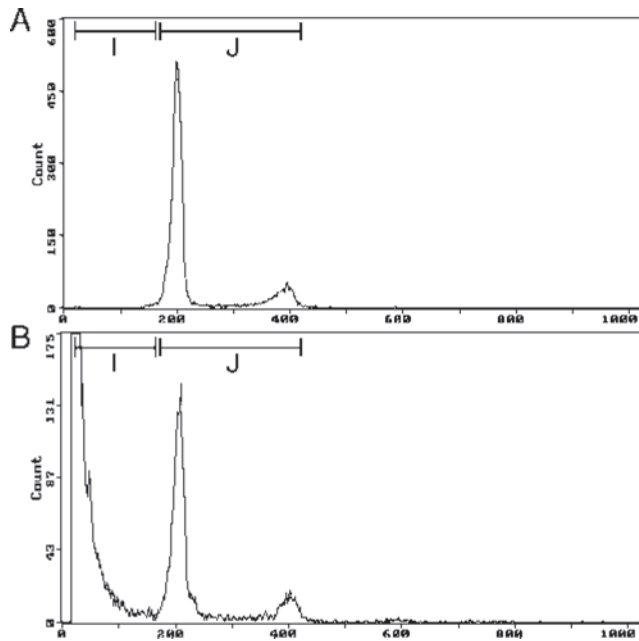


Figure 1 Histograms obtained after PI labeling and flow cytometry analysis of astrocytes at 72 h after *ts1* infection. I identifies the sub-G1 peak, containing apoptotic cells, and J identifies cell populations whose DNA content correlates with the normal cell cycle. **A**, Control astrocytes. **B**, Infected astrocytes.

of infected C1 astrocytes showed typical apoptotic changes, such as nuclear condensation (Figure 2B, C, D) and fragmentation (Figure 2C, D) at 48 and 72 h p.i. In the infected cell cultures, percentages of cells having apoptotic nuclei increased in a time-dependent manner (from 48 to 72 h p.i.). Notably, most of the apoptotic nuclei appeared to be in multinucleated syncytia (which commonly form in C1 cell cultures infected with *ts1*). Although apoptotic nuclei were evident both at 48 and 72 h p.i., PI-stained nuclei (as

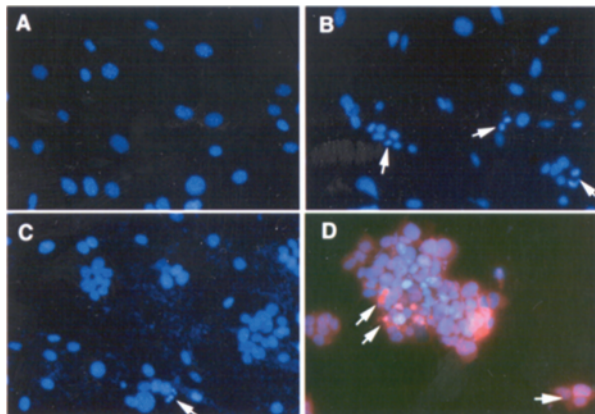


Figure 2 Nuclear staining in astrocytes by Hoechst 33342 and PI. **A**, Control astrocytes. **B** and **C**, Infected astrocytes at 48 h post infection. **D**, Infected astrocytes at 72 h post infection. Note DNA condensation and fragmentation (arrows in **B** and **C**), and PI positive cells (arrows in **D**).

an indication of a later stage of apoptosis or necrosis) were rare at 48 h p.i., becoming more common by 72 h p.i. (Figure 2D). Similar results were observed by using primary cultured astrocytes, or PCAs (data not shown).

ts1 infection triggers ER stress in astrocytes

In many other systems and cell types, the UPR is initiated by the activation of the ER transmembrane kinases IRE1 and PERK (Bertolotti *et al*, 2000; Shamu and Walter, 1996). In mammalian cells, IRE1 activation might not be necessary for UPR signal transduction (Urano *et al*, 2000). To determine whether the accumulation of abnormal gPr80^{env} elicits an authentic UPR in *ts1*-infected astrocytes, we compared uninfected to *ts1*-infected C1 cells for downstream effectors (including eIF2 α , chaperones, and GADD153) that are modulated by PERK activation. The hallmark of ER stress-induced apoptosis is cleavage and activation of the ER membrane-associated cysteine protease, procaspase-12 (Nakagawa *et al*, 2000; Rao *et al*, 2001). To determine whether caspase-12 activation is involved in apoptosis in *ts1*-infected C1, we also performed Western blot analyses using an antibody that detects procaspase-12.

As shown in Figure 3, the amounts of phosphorylated eIF2 α in infected C1 cells increased from 8 h p.i. (data not shown), through 24, 48, and 72 h p.i., as did GADD153. Amounts of the chaperone GRP78 were increased as early as 24 h p.i. in infected C1 cells, and levels of this protein remained consistently higher in infected cells, relative to control cells, through 72 h p.i. At 48 and 72 h p.i., the amount of procaspase-12 was decreased in infected C1 cells relative to controls, reflecting the cleavage and activation of this enzyme.

Because the C1 astrocyte cell line contains the SV-40 large T antigen, which may complicate cell responses to virus infection, we also performed studies in PCAs. As shown in Figure 4, 72 h p.i., levels of GRP78 in PCAs were increased, and procaspase-12 (55 kDa) was cleaved into activated form (40 kDa).

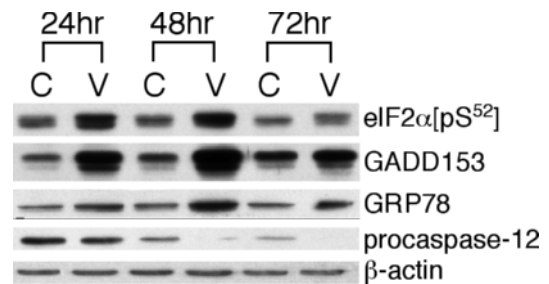


Figure 3 Effects of *ts1* infection on the levels of eIF2 α [pS⁵²], GADD153, GRP78, and procaspase-12 in C1 cells. C1 cells were infected with *ts1* at a MOI of 10 for 40 min in 100-mm dishes, and cells were harvested at different times after infection. C identifies uninfected C1 cells and V identifies *ts1*-infected C1 cells. After imaging, the same blots were stripped and reimblotted with anti- β -actin antibody as a protein loading control. Blots shown are representative of four independent experiments.

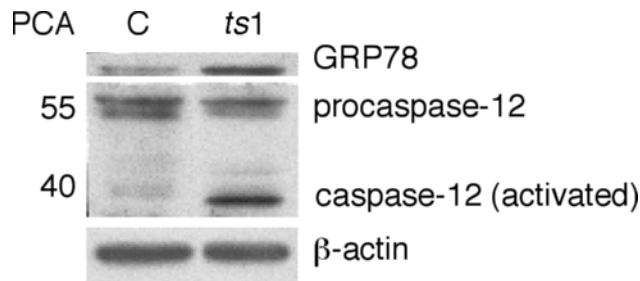


Figure 4 Effects of *ts1* infection on the levels of GRP 78, procaspase-12, and activated caspase-12 in primary cultured astrocytes (PCA). PCA were infected with *ts1* at a MOI of 10 for 4 h in 100-mm dishes, and cells were harvested at 3 days after infection. C identifies uninfected control and *ts1* identifies *ts1*-infected PCA. After imaging, the same blots were stripped and reimmunoblotted with anti- β -actin antibody as a protein loading control. Blots shown are representative of two independent experiments.

The similarity between these results with PCAs (Figure 4) and results from C1 cells (Figure 3) suggests that C1 cells retain the characteristics of PCAs, and that *ts1*-induced ER stress responses are similar in both PCAs and C1 cells.

ts1 induces a mitochondrial stress response in astrocytes

Recent work from several laboratories has shown that the ER stress signals are transmitted to mitochondria via mechanisms that include mitochondrial Ca^{2+} loading from the ER, Bcl-2 regulation, and ROS overproduction (Hacki *et al*, 2000; Hori *et al*, 2002; Jacobson and Duchen, 2000; Nakamura *et al*, 2000). Thus it is of great interest to determine whether a mitochondrial stress response follows ER stress in *ts1* infection. The mitochondrial stress response culminates in outer and inner membrane permeabilization, which leads to cytochrome *c* release, caspase-9 activation, and $\Delta\Psi_m$ dissipation.

To detect changes in $\Delta\Psi_m$ after *ts1* infection, we used the JC-1 fluorescent staining technique, which employs an indicator dye to distinguish between cells with orange mitochondria (normal $\Delta\Psi_m$) from cells with green cytoplasm (loss of $\Delta\Psi_m$), as described in Materials and Methods. Figure 5 shows that percentages of cells with orange mitochondria relative to total cells (orange + green) were significantly decreased in *ts1*-infected C1 cells, relative to uninfected cells, by 48 h p.i. ($P < .01$, compared to that of control group). There was no significant difference between infected and uninfected cells at 24 h p.i. (data not shown). Similar results were detected by using PCAs (data not shown).

In cells undergoing mitochondrial stress, apoptotic events downstream of mitochondrial outer membrane permeabilization is cytochrome *c* release from mitochondria (Li *et al*, 1997). Cytosolic cytochrome *c* forms an apoptosome, which is composed of cytochrome *c*, Apaf-1, and procaspase-9. The result of apoptosome formation is cleavage of procaspase-9 into activated caspases-9. Activated caspase-9 then

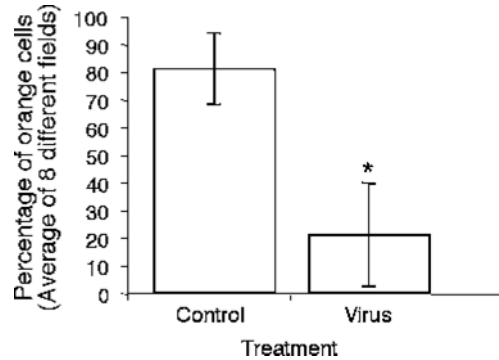


Figure 5 Effects of *ts1* infection on mitochondrial transmembrane potentials ($\Delta\Psi_m$) in C1 cells. C1 cells were infected with *ts1* at a MOI of 10 for 40 min in 100-mm dishes. At 48 h post infection, cells were stained with JC-1. $\Delta\Psi_m$ dissipation was indicated as green cytoplasmic fluorescence, compared to normal $\Delta\Psi_m$ as orange fluorescence in the mitochondria. The graph shows the average percentages of cells with orange mitochondria (of total cells) for eight random fields in uninfected (Control) and *ts1*-infected C1 (Virus) cells at 48 h post infection. * $P < .01$ for control versus infected C1 cells.

processes and activates caspase-3, which executes apoptosis of cells. Figure 6 shows that procaspase-9 and procaspase-3 (35 kDa) are cleaved in *ts1*-infected C1 cells, and activated caspase-3 (17 kDa) is increased. Both changes were evident by 48 and 72 h p.i., but not at 24 h p.i.

Expression of activated caspase-3 in brainstems of *ts1*-infected mice

To determine whether caspase-3-related apoptosis participates in neurodegeneration in *ts1*-infected mice, we identified and localized activated caspase-3 using immunohistochemistry in sections of brainstem from infected and uninfected animals. Figure 7 shows that brainstem sections of *ts1*-infected animals contained significantly increased amounts of activated caspase-3 by 25 days p.i. ($P < .01$), compared to sections from uninfected controls. In sections from infected animals, the antibody identified activated caspase-3 in astrocytes and neurons, with most caspase-3-positive astrocytes found surrounding

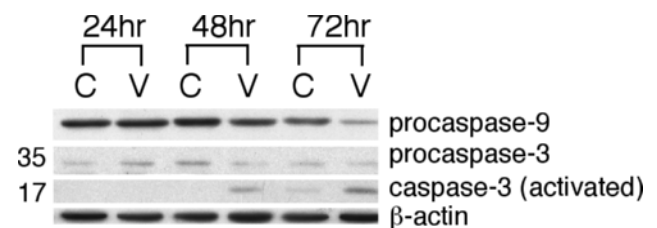


Figure 6 Effects of *ts1* infection on the levels of procaspase-9, procaspase-3, and activated caspase-3 in C1 cells. C1 cells were infected with *ts1* at a MOI of 10 for 40 min in 100-mm dishes, and cells were harvested at different times after infection. C identifies uninfected C1 cells and V identifies *ts1*-infected C1 cells. After imaging, the same blots were stripped and immunoblotted with anti- β -actin antibody as a protein loading control. Blots shown are representative of four independent experiments.

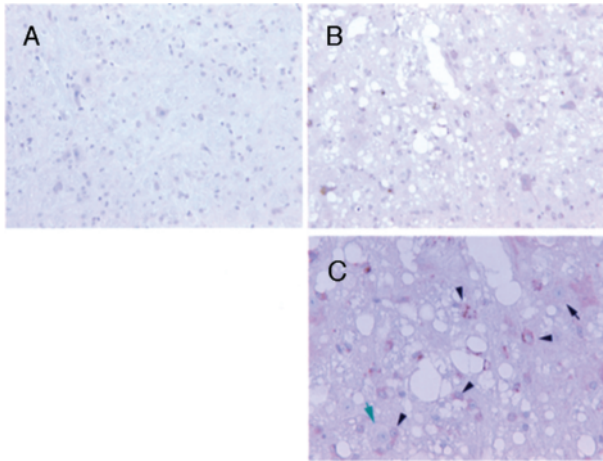


Figure 7 Expression of activated caspase-3 protein in brainstem cells of control and *ts1*-infected mice at 25 days post infection. **A**, Caspase-3 immunoreactivity (brown) in the cytoplasm of brainstem astrocytes and neurons from a control mouse. **B**, Caspase-3 immunoreactivity (brown) in the cytoplasm of brain stem astrocytes and neurons from a *ts1*-infected mouse. **C**, Higher magnification of the astrocytes and neurons in panel **B**. Note the strong brown staining in astrocytes (black arrowhead) and neurons (black arrow), and caspase-3-positive astrocytes surrounding the degenerated neuron (green arrow).

degenerated neurons within the areas of spongiform lesions (Figure 7).

Mitochondrial lesions in astrocytes from the brainstem in infected mice

To determine whether *ts1*-induced neurodegeneration is associated with mitochondrial damage, we used transmission electron microscopy to examine mitochondria in astrocytes of brainstem sections from *ts1*-infected mice (25 days p.i.). As shown in Figure 8A, swollen mitochondria are found in astrocytes of infected brainstem tissue, and some mito-

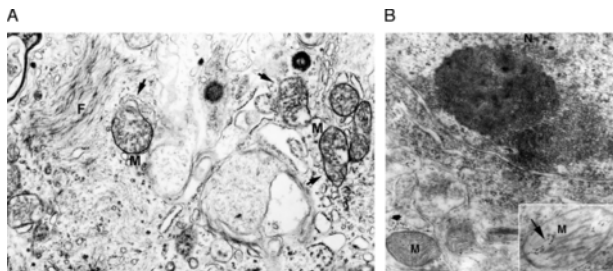


Figure 8 Electron micrographs showing mitochondrial swelling and degeneration in astrocytes from brainstem tissue of *ts1*-infected mice. **A**, An astrocyte from a spongiform lesion in the brainstem of a *ts1*-infected mouse sacrificed at 25 days post infection. Arrows point to mitochondria, which are swollen and disintegrated. F denotes glial fibrillary acidic protein, which identifies the cell as an astrocyte. **B**, An astrocyte from a spongiform lesion in the brainstem of a *ts1*-infected mouse sacrificed at 25 days post infection. The arrow points to a damaged mitochondrion (inset) with granular calcium pyroantimonate deposits. M marks mitochondria, and N marks the nucleus. (25,000 \times)

chondria are completely disintegrated. In brainstems processed by the pyroantimonate method for detection of precipitated calcium, granular calcium pyroantimonate deposits are evident in astrocyte mitochondria in sections from infected animals (Figure 8B).

Discussion

In this time-course study of *ts1*-infected astrocytes, we have identified two specific intracellular pathways (ER stress and mitochondrial stress) that contribute to apoptosis after infection. Soon after *ts1* infection of C1 cells (8 h p.i.), a UPR is initiated, as evidenced by PERK activation. PERK activation was detected by means of its downstream events, which include (a) hyperphosphorylation of eIF2 α , (b) induction of GADD153/CHOP, and (c) up-regulation of GRP78 (Figure 3). In a recently submitted paper, we have also shown that UPR-induced IRE1 activation occurs after *ts1* infection, as indicated by activation of the IRE1-JNK cascade (Kim *et al*, submitted). In another communication, we have documented that *ts1* infection in astrocytes induces activation of NF κ B by degradation of I κ B (Kim *et al*, 2001), suggesting that an EOR response is also activated in *ts1*-infected cells. Together these data provide strong evidence that ER stress responses (UPR and EOR) are activated by *ts1* infection in C1 cells.

Because ER stress induces GADD153 expression via PERK activation (Figure 3), it is important to note that GADD153 sensitizes cells to ER stress and promotes ROS production by down-regulating Bcl-2 production and reducing intracellular glutathione (GSH) levels (McCullough *et al*, 2001). In *ts1* infection, we have shown that oxidative stress is involved in the death of cultured astrocytes (Liu *et al*, 2002), and our more recent work has shown that Bcl-2 down-regulation and GSH depletion occur in the infected cells (data not shown). In light of these observations, it seems likely that GADD153 up-regulation contributes to the profound redox imbalance that follows *ts1* infection in C1 astrocytes.

Recent investigations into the apoptotic process have identified mechanisms by which cell stress signals are transmitted from the ER to mitochondria. Chemicals that change protein structure and provoke protein accumulation in the ER (such as brefeldin and tunicamycin), cause ER stress and subsequent mitochondrial stress, as shown by cytochrome *c* release and caspase-3 activation (Hacki *et al*, 2000). In the present study, mitochondrial stress following ER stress was detected by $\Delta\Psi_m$ dissipation and procaspase-9 cleavage at 48 h p.i. (Figures 5, 6). Possible routes for signaling between the ER and mitochondria in *ts1* infection are now under investigation.

In *ts1*-infected C1 cells, events that precede apoptosis include the activation of specific marker enzymes for ER and mitochondrial stress, including

caspase-12, caspase-9, and caspase-3 (Figures 3, 6). In light of these findings, we infer that both ER-related and mitochondria-related apoptotic pathways participate in astrocyte apoptosis caused by *ts1*.

In brain spongiform lesions caused by *ts1*, neuronal loss and gliosis are more prominent histologically than is astrocyte apoptosis (Stoica *et al*, 1993, 2000). We have observed that caspase-3 activation and mitochondrial damage occur in astrocytes from brainstems of *ts1*-infected mice, and that the cells showing such changes are associated with spongiform lesions (Figures 7, 8). Because our cultured astrocytes are infected with a relatively high concentration of virus, and because *in vivo* infection of the brainstem requires viral passage across the blood-brain barrier, it is not surprising that astrocyte apoptosis is an obvious and common outcome for cells infected *in vitro*, whereas *in vivo* astrocyte infection may not always result in cell death.

In *ts1* infection and in HIV infection, glial cells of the central nervous system are infected by the virus, but neurons are not (Gonzales-Scarano *et al*, 1995; Kaul *et al*, 2001; Stoica *et al*, 1993; Wong *et al*, 1998). In both cases, this would imply that neuronal death may be due to events occurring in the surrounding infected cells. In this study, we have shown that *ts1*-infected astrocytes are under ER stress and mitochondrial stress, and our previous work has documented NF κ B activation in *ts1*-infected astrocytes (Kim *et al*, 2001). ER stress causes NF κ B translocation, which activates transcription of downstream cytokines and inflammatory factors (such as interleukin [IL]-1, IL-6, iNOS, and TNF α). After *ts1*-infection, Fas and TNF α expression are increased in astrocytes from infected mice (Choe *et al*, 1998), and iNOS expression is up-regulated in infected astrocytes in culture (Kim *et al*, 2001). Increased production and release of these factors from astrocytes is therefore likely to damage nearby neurons (Kaul *et al*, 2001). Injury to astrocytes by *ts1* infection would likely impair the glutamate EAAT2 transporter, leading to accumulation of glutamate in the extracellular space with secondary excitotoxic damage contributing to neuronal degeneration (Danbolt, 2001). In HIV infection, NF κ B activation in astrocytes contributes to reactive astrogliosis (Ghorpade *et al*, 2003), and in scrapie infected mice, PrP^{Sc} accumulates in astrocytes rather than neurons, and these events precede astrogliosis and neuronal loss (Diedrich *et al*, 1991). Together these observations implicate ER stress or NF κ B activation in astrocytes as a cause of reactive astrogliosis. Furthermore, ER stress and mitochondrial stress also promote ROS production in these cells by means of GADD153 activation and mitochondrial dysfunction (Liu *et al*, 2002; McCullough *et al*, 2001; Kroemer and Reed, 2000). A recent study has shown that astrocytes have stronger antioxidative potential than neurons, and can protect neurons from oxidative stress (Shih *et al*, 2003). In *ts1*-infected mice, infected astrocytes may contribute to neurodegeneration in several

ways, e.g., (a) releasing neurotoxins, (b) accumulation of glutamate due to impairment of the EAAT2 transporter, (c) promoting astrogliosis (Hori *et al*, 2002), and (d) failing to provide redox support to neurons, all of which could conceivably occur without extensive astrocyte loss by apoptosis.

Several animal viruses have been shown to encode proteins that disturb the ER-Golgi secretory pathway, and cause ER stress, in host cells. These include FrCas^E (Dimcheff *et al*, 2003), Japanese encephalitis virus (Su *et al*, 2002), bovine diarrhea virus (Jordan *et al*, 2002), and hepatitis C virus (Waris *et al*, 2002). The results reported here are the first to show that infection in astrocytes by a retrovirus (with accumulation of viral proteins in the ER) can have similar effects, causing ER and mitochondrial stress responses. Because the *ts1* mouse develops a neuroimmunodegenerative syndrome similar to that following HIV-1 infection in humans, it is interesting to note that the HIV-1 envelope preprotein gp160 accumulates in the ER in infected cells, due to its very slow transit through this compartment (Crise *et al*, 1990; Koga *et al*, 1990; Crise and Rose, 1992; Land *et al*, 2003). This observation opens the novel possibility that the cell type-specific cytopathic and apoptotic effects of HIV-1, like those of *ts1*, may involve ER and mitochondrial stress pathways resulting directly from viral preprotein accumulation in infected cells.

Several neurodegenerative diseases not caused by viruses, including Alzheimer's disease, Parkinson's disease, amyotrophic lateral sclerosis, and prion diseases, have also been shown to involve abnormal processing and retention of specific proteins in the ER (Diedrich *et al*, 1991; Aridor and Hannan, 2000; Imaizumi *et al*, 2001; Kudo *et al*, 2002; Hetz *et al*, 2003). Like the gPr80^{env} aggregates that accumulate in *ts1*-infected astrocytes, these proteins may cause neurodegenerative disease by triggering cytopathic events and apoptosis in cells of the central nervous system. The data presented here form the foundation for our current *in vivo* tests of ER stress- and mitochondrial stress-targeted drug treatments of *ts1*-induced neurodegeneration.

Materials and methods

Materials

Dulbecco's modified Eagle's medium (DMEM), fetal bovine serum (FBS), penicillin, streptomycin, and trypsin were from Invitrogen Life Technologies (Carlsbad, CA, USA). All other reagents, unless specifically described, were obtained from Sigma Chemical (St Louis, MO, USA).

Astrocyte preparation

Primary cortical astrocytes were isolated from 1- to 2-day-old FVB mice by a modification of methods described previously (Liu *et al*, 2002). The cells were plated onto poly-L-lysine-coated flasks and grown in

DMEM/F12 medium supplemented with 10% FBS, 100 U/ml penicillin, 100 $\mu\text{g/ml}$ streptomycin, and 2.5 $\mu\text{g/ml}$ fungizone for 7 to 9 days, until reaching confluence. The cells were then passaged four to five times before use. These cultures contained more than 85% glial fibrillary acidic protein (GFAP)-positive cells, as detected using rabbit anti-mouse GFAP antibody (DAKO, Carpinteria, CA, USA).

The C1 astrocyte cell line was established previously by immortalizing primary murine astrocytes with the SV-40 large T antigen (Lin *et al*, 1997). The C1 line maintains most of the characteristics of primary astrocytes (Lin *et al*, 1997). For this study, C1 cells were grown in DMEM medium supplemented with 10% FBS, 100 IU/ml penicillin, and 100 $\mu\text{g/ml}$ streptomycin at 37°C in a humidified atmosphere of 5% CO₂ in air.

ts1 infection of astrocytes and treatment

Astrocytes were seeded in 60-mm or 100-mm plastic tissue culture dishes. The next day, C1 cells were incubated for 1 h before infection in DMEM medium containing 1% FBS and 3 $\mu\text{g/ml}$ polybrene (to enhance viral absorption), while PCAs were incubated for 1 h before infection in DMEM/F12 medium containing 1% FBS and 10 $\mu\text{g/ml}$ polybrene. The cells were then infected with *ts1* for 40 min (C1 cells), or 4 h (PCAs), at 34°C, using a multiplicity of infection (MOI) of 10 (in mediums containing polybrene, as before). The cells were then washed and re-fed with fresh medium containing 10% FBS, and were incubated at 37°C in a humidified atmosphere of 5% CO₂ in air. The treated and control cultures were harvested at different time points post infection for analysis by JC-1 staining, flow cytometry, Western blotting, and Hoechst staining (below).

JC-1 staining

For JC-1 staining, C1 cells were grown in 100-mm culture dishes. A stock solution of JC-1 (5,5',6,6'-tetrachloro-1,1',3,3'-tetraethylbenzimidazolylcarbocyanine chloride, from BioVision, Mountain View, CA) was made at 1 mg/ml in dimethylsulfoxide, and fresh staining solution (1 $\mu\text{g/ml}$) was prepared by diluting the stock solution in warm (37°C) culture medium supplemented with 10% FBS (staining medium). For staining, 5 ml of staining medium was used for each dish, and the dishes were incubated for 10 min in a cell culture incubator (in the dark). The treated cells were then rinsed three times in warm dye-free phosphate-buffered saline (PBS) (pH 7.4), and overlaid with 1 ml of culture medium for viewing under the fluorescence microscope. In healthy cells with normal $\Delta\Psi_m$, the JC-1 dye localizes to the mitochondria, where it aggregates and is visualized as bright orange fluorescence. In cells whose mitochondria have been damaged (with $\Delta\Psi_m$ dissipation), JC-1 does not aggregate in the mitochondria, but instead appears as bright green fluorescence in the cytoplasm. Uninfected and

infected cell cultures were stained at 24 and 48 h p.i., and eight fields were chosen randomly from the stained plates for photomicrography. For each image, the numbers of orange cells *versus* green cells were counted by an observer who was blinded to the identity of the culture (control *versus* infected). Average percentages of orange cells (relative to the total cell number) were compared for control *versus* infected cells at each time point.

Flow cytometry analysis

Cultured C1 cells were gently trypsinized and removed from the culture dishes. The suspended cells were fixed in 70% ethanol and stained with PI containing RNase (DNase-free, from Roche). DNA content was then analyzed by flow cytometry on a Coulter Epics Elite flow cytometer. Apoptotic cells (the "sub-G1 peak") were detected in a distinct peak with lower fluorescence intensity than the normal cells. Necrotic fragments were excluded by appropriate gate and marker positioning (Micoud *et al*, 2001).

Hoechst 33342 and PI staining

C1 cell cultures growing in 100-mm culture dishes were incubated for 30 min in the dark in culture medium containing 1 $\mu\text{g/ml}$ of Hoechst 33342 and 1 $\mu\text{g/ml}$ of PI. The cell cultures were then rinsed three times in culture medium without dye, and overlaid with 1 ml of culture medium for viewing and photography under the fluorescent microscope.

Western blot analysis

C1 cells were harvested and total proteins isolated using RIPA buffer (1% NP40, 0.5% sodium deoxycholate, 0.1% sodium dodecyl sulfate [SDS], 0.25 mM phenylmethylsulfonyl fluoride [PMSF], 1 mM sodium fluoride in PBS), supplemented with a protease inhibitor cocktail (Sigma), according to a modified protocol described previously (Liu *et al*, 2002). Protein concentrations were measured using Bio-Rad D_C Protein Assay Reagent (BioRad Laboratories) following the manufacturer's suggestions. Fifty micrograms of protein from cell lysates was separated by 12% SDS-PAGE. After electrophoresis, the proteins were transferred to a PVDF membrane (Millipore). The membrane was blocked for 1 h in Tris-buffered saline (TBS) with 5% nonfat milk at room temperature, and then immunoblotted with antibodies against activated caspase-3, procaspase-9, procaspase-12 (BioVision), procaspase-3 (Cell Signaling), GADD153, GRP78 (Santa Cruz), and phosphospecific eIF2 α [pS⁵²] (this antibody specifically recognizes phosphorylated eIF2 α at Ser-52, from Biosource). Afterward, the membranes were incubated with horseradish peroxidase-conjugated secondary antibodies, and immune complexes were detected by chemiluminescence (NEN Life Science Products).

Animal treatment

Newborn pups were infected intraperitoneally with *ts1*, and control uninfected pups received the same volume of culture medium without virus. The titer of all *ts1* inocula used in this study was 1.7×10^7 infectious units/ml. Treated and control pups within individual experiments were from the same litter.

Immunohistochemistry

Immunohistochemistry was performed as described previously (Kim *et al*, 2000). Briefly, *ts1*-infected ($n = 5$) and control ($n = 5$) mice were anesthetized at 25 days p.i. by intraperitoneal injection of pentobarbital (150 mg/kg), and then were transcardially perfused with 10% buffered formalin as a fixative using a peristaltic pump. After 12 h of fixation, each mouse's brain was dissected, with the brainstem segments separated for further processing.

For localization of activated (cleaved) caspase-3 in cells of the brainstem, paraffin-embedded sections (6 μm) were first deparaffinized and washed with Tris-buffered saline (TBS; 100 mM Tris, 150 mM NaCl, pH 7.4) for 20 min at room temperature. The sections were then subjected to an antigen retrieval protocol, in which they were heated in 10 mM citrate buffer (pH 6.0) for 10 min, blocked with 5% normal goat serum in TBS, and then incubated overnight at 4°C with rabbit anti-activated caspase-3 antibody (Cell Signaling) at a dilution of 1:100. After three 5-min washes in TBS, the sections were incubated with biotin-conjugated anti-rabbit immunoglobulin G (IgG) for 30 min at room temperature, and then treated with reagents from a Vecta-Elite streptavidin-peroxidase kit with a benzidine substrate for color development. The sections were counterstained with 1% methyl green or diluted hematoxylin. Sections that were not incubated with a primary antibody served as negative controls.

Transmission electron microscopy

For electron microscopy of brainstem sections, six mice from the same litter were used. Three of the mice were infected with *ts1*, and three served as uninfected controls, as previously described (Stoica *et al*, 2000). The infected and control mice were anesthetized at 25 days p.i. with an intraperitoneal injection of pentobarbital (150 mg/kg), and perfused via the left ventricle with heparin (9 mg/L in saline), followed

by 2% paraformaldehyde and 2% glutaraldehyde in 0.1 M cacodylate buffer (pH 7.2). The brainstems were dissected and cut into 1.0-mm³ cubes, washed twice in cacodylate buffer, and postfixed in 1.3% osmium tetroxide in S-collidine (pH 7.4). The fixed tissue blocks were then dehydrated through gradient concentrations of ethanol, transferred to propylene oxide, and embedded in Epon/Araldite. One-micrometer sections were cut with glass knives and stained with toluidine blue (0.1% aqueous solution). Thin sections for ultrastructural evaluation were cut on an LKB ultramicrotome with a diamond knife, stained with uranyl acetate and lead citrate, and examined under a Zeiss 10 electron microscope.

Ultrastructural localization of calcium

The oxalate-pyroantimonate procedure was used to visualize the subcellular distribution of calcium in cells from mouse brainstem tissues, as described by Siklos *et al* (2000). The infected and uninfected mice were sacrificed at 25 days p.i. (with three infected and three serving as controls from the same litters). The experimental animals were perfused overnight at 4°C with a solution containing 2% paraformaldehyde, 2% glutaraldehyde, and 90 mM potassium oxalate (pH 7.4). The brainstems were then removed and washed for 15 min in 7.5% sucrose containing 90 mM potassium oxalate, and postfixed for 2 h in a mixture of 1% osmium tetroxide and 2% potassium pyroantimonate in 0.01 N acetic acid (adjusted to pH 7.4 with 0.4 N potassium hydroxide). After a short rinse in cold distilled water brought to pH 10 with potassium hydroxide, the brainstems were dehydrated in a graded series of ethanol, embedded in Araldite, and sectioned for conventional microscopy (semithin sections stained with 1% toluidine blue) or for electron microscopy (ultrathin sections prepared on a Reichert OMU 2 ultramicrotome). The ultrathin sections were stained with 0.5% uranyl acetate and 0.4% lead citrate and examined with a Zeiss EM 10 electron microscope.

Statistical analysis

Data are presented as mean \pm SD. The statistical significance of the results was determined by Student's *t* test. A probability of less than 5% was considered significant.

References

- Aridor M, Hannan LA (2000). Traffic jam: a compendium of human diseases that affect intracellular transport processes. *Traffic* **1**: 836–851.
- Atwood WJ, Berger JR, Kaderman R, Tornatore CS, Major EO (1993). Human immunodeficiency virus type 1 infection of the brain. *Clin Microbiol Rev* **6**: 339–366.
- Baeuerle PA, Baichwal VR (1997). NF-kappa B as a frequent target for immunosuppressive and anti-inflammatory molecules. *Adv Immunol* **65**: 111–137.
- Bertolotti A, Zhang Y, Hendershot LM, Harding HP, Ron D (2000). Dynamic interaction of BiP and ER stress transducers in the unfolded-protein response. *Nat Cell Biol* **2**: 326–332.
- Brack-Werner R (1999). Astrocytes: HIV cellular reservoirs and important participants in neuropathogenesis. *AIDS* **13**: 1–22.
- Clark S, Duggan J, Chakraborty J (2001). Ts1 and LP-BM5: a comparison of two murine retrovirus models for HIV. *Viral Immunol* **14**: 95–109.

- Crise B, Buonocore L, Rose JK (1990). CD4 is retained in the endoplasmic reticulum by the human immunodeficiency virus type 1 glycoprotein precursor. *J Virol* **64**: 5585–5593.
- Crise B, Rose JK (1992). Human immunodeficiency virus type 1 glycoprotein precursor retains a CD4-p56lck complex in the endoplasmic reticulum. *J Virol* **66**: 2296–2301.
- Choe W, Stoica G, Lynn W, Wong PKY (1998). Neurodegeneration induced by MoMuLV-ts1 and increased expression of Fas and TNF-alpha in the central nervous system. *Brain Res* **779**: 1–8.
- Danbolt NC (2001). Glutamate uptake. *Prog Neurobiol* **65**: 1–105.
- Diedrich JF, Bendheim PE, Kim YS, Carp RI, Haase AT (1991). Scrapie associated prion protein accumulates in astrocytes during scrapie infection. *Proc Natl Acad Sci U S A* **88**: 375–379.
- Dimcheff DE, Askovic S, Baker AH, Johnson-Fowler C, Portis JL (2003). Endoplasmic reticulum stress is a determinant of retrovirus-induced spongiform neurodegeneration. *J Virol* **77**: 12617–12629.
- Duchen MR (2000). Mitochondria and calcium: from cell signalling to cell death. *J Physiol* **529(Pt 1)**: 57–68.
- Friedlander RM (2003). Apoptosis and caspases in neurodegenerative diseases. *N Engl J Med* **348**: 1365–1375.
- Galey D, Becker K, Haughey N, Kalehua A, Taub D, Woodward J, Mattson MP, Nath A (2003). Differential transcriptional regulation by human immunodeficiency virus type 1 and gp120 in human astrocytes. *J NeuroVirol* **9**: 358–371.
- Gonzales-Scarano F, Nathanson N, Wong PKY (1995). Retroviruses and the nervous system. In: *The Retroviridae*, vol. 4. Levy JA (ed). New York: Plenum Press, pp 409–490.
- Ghorpade A, Holter S, Borgmann K, Persidsky R, Wu L (2003). HIV-1 and IL-1 beta regulate Fas ligand expression in human astrocytes through the NF-kappa B pathway. *J Neuroimmunol* **141**: 141–149.
- Hacki J, Egger L, Monney L, Conus S, Rosse T, Fellay I, Borner C (2000). Apoptotic crosstalk between the endoplasmic reticulum and mitochondria controlled by Bcl-2. *Oncogene* **19**: 2286–2295.
- Harding HP, Zhang Y, Bertolotti A, Zeng H, Ron D (2000). Perk is essential for translational regulation and cell survival during the unfolded protein response. *Mol Cell* **5**: 897–904.
- Hetz C, Russelakis-Carneiro M, Maundrell K, Castilla J, Soto C (2003). Caspase-12 and endoplasmic reticulum stress mediate neurotoxicity of pathological prion protein. *EMBO J* **22**: 5435–5445.
- Hori O, Ichinoda F, Tamatani T, Yamaguchi A, Sato N, Ozawa K, Kitao Y, Miyazaki M, Harding HP, Ron D, Tohyama M, Stern DM, Ogawa S (2002). Transmission of cell stress from endoplasmic reticulum to mitochondria: enhanced expression of Lon protease. *J Cell Biol* **157**: 1151–1160.
- Imaizumi K, Miyoshi K, Katayama T, Yoneda T, Taniguchi M, Kudo T, Tohyama M (2001). The unfolded protein response and Alzheimer's disease. *Biochem Biophys Acta* **1536**: 85–96.
- Jacobson J, Duchon MR (2002). Mitochondrial oxidative stress and cell death in astrocytes—requirement for stored Ca²⁺ and sustained opening of the permeability transition pore. *J Cell Sci* **115**: 1175–1188.
- Jordan R, Wang L, Graczyk TM, Block TM, Romano PR (2002). Replication of a cytopathic strain of bovine viral diarrhoea virus activates PERK and induces endoplasmic reticulum stress-mediated apoptosis of MDBK cells. *J Virol* **76**: 9588–9599.
- Kaul M, Garden GA, Lipton SA (2001). Pathways to neuronal injury and apoptosis in HIV-associated dementia. *Nature* **410**: 988–994.
- Kim HT, Qiang W, Wong PKY, Stoica G (2001). Enhanced proteolysis of IkappaBalpha and IkappaBbeta proteins in astrocytes by Moloney murine leukemia virus (MoMuLV)-ts1 infection: a potential mechanism of NF-kappaB activation. *J NeuroVirol* **7**: 466–475.
- Kim HT, Stoica G, Bazer FW, Ott TL (2000). Interferon tau-induced hepatocyte apoptosis in sheep. *Hepatology* **31**: 1275–1284.
- Koga Y, Sasaki M, Nakamura K, Kimura G, Nomoto K (1990). Intracellular distribution of the envelope glycoprotein of human immunodeficiency virus and its role in the production of cytopathic effect in CD4+ and CD4–human cell lines. *J Virol* **64**: 4661–4671.
- Kozutsumi Y, Segal M, Normington K, Gething MJ, Sambrook J (1988). The presence of malformed proteins in the endoplasmic reticulum signals the induction of glucose-regulated proteins. *Nature* **332**: 462–464.
- Kroemer G, Reed JC (2000). Mitochondrial control of cell death. *Nat Med* **6**: 513–519.
- Kudo T, Katayama T, Imaizumi K, Yasuda Y, Yatera M, Okochi M, Tohyama M, Takeda M (2002). The unfolded protein response is involved in the pathology of Alzheimer's disease. *Ann N Y Acad Sci* **977**: 349–355.
- Land A, Zonneveld D, Braakman I (2003). Folding of HIV-1 envelope glycoprotein involves extensive isomerization of disulfide bonds and conformation-dependent leader peptide cleavage. *FASEB J* **17**: 1058–1067.
- Li P, Nijhawan D, Budihardjo I, Srinivasula SM, Ahmad M, Alnemri ES, Wang X (1997). Cytochrome c and dATP-dependent formation of Apaf-1/caspase-9 complex initiates an apoptotic protease cascade. *Cell* **91**: 479–489.
- Lin YC, Chow CW, Yuen PH, Wong PKY (1997). Establishment and characterization of conditionally immortalized astrocytes to study their interaction with ts1, a neuropathogenic mutant of Moloney murine leukemia virus. *J NeuroVirol* **3**: 28–37.
- Liu N, Qiang W, Kuang X, Thuillier P, Lynn WS, Wong PKY (2002). The peroxisome proliferator phenylbutyric acid (PBA) protects astrocytes from ts1 MoMuLV-induced oxidative cell death. *J NeuroVirol* **8**: 318–325.
- May MJ, Ghosh S (1998). Signal transduction through NF-kappa B. *Immunol Today* **19**: 80–88.
- McCullough KD, Martindale JL, Klotz LO, Aw TY, Holbrook NJ (2001). Gadd153 sensitizes cells to endoplasmic reticulum stress by down-regulating Bcl2 and perturbing the cellular redox state. *Mol Cell Biol* **21**: 1249–1259.
- Micoud F, Mandrand B, Malcus-Vocanson C (2001). Comparison of several techniques for the detection of apoptotic astrocytes in vitro. *Cell Prolif* **34**: 99–113.
- Mourelatos Z, Hirano A, Rosenquist AC, Gonatas NK (1994). Fragmentation of the Golgi apparatus of motor neurons in amyotrophic lateral sclerosis (ALS). Clinical studies in ALS of Guam and experimental studies in deafferented neurons and in beta,beta'-iminodipropionitrile axonopathy. *Am J Pathol* **144**: 1288–1300.
- Nakagawa T, Zhu H, Morishima N, Li E, Xu J, Yankner BA, Yuan J (2000). Caspase-12 mediates

- endoplasmic-reticulum-specific apoptosis and cytotoxicity by amyloid-beta. *Nature* **403**: 98–103.
- Nakamura K, Bossy-Wetzel E, Burns K, Fadel MP, Lozyk M, Goping IS, Opas M, Bleackley RC, Green DR, Michalak M (2000). Changes in endoplasmic reticulum luminal environment affect cell sensitivity to apoptosis. *J Cell Biol* **150**: 731–740.
- Pahl HL, Baeuerle PA (1996). Activation of NF-kappa B by ER stress requires both Ca²⁺ and reactive oxygen intermediates as messengers. *FEBS Lett* **392**: 129–136.
- Rao RV, Hermel E, Castro-Obregon S, del Rio G, Ellerby LM, Ellerby HM, Bredesen DE (2001). Coupling endoplasmic reticulum stress to the cell death program. Mechanism of caspase activation. *J Biol Chem* **276**: 33869–33874.
- Shamu CE, Walter P (1996). Oligomerization and phosphorylation of the Ire1p kinase during intracellular signaling from the endoplasmic reticulum to the nucleus. *EMBO J* **15**: 3028–3039.
- Shih AY, Johnson DA, Wong G, Kraft AD, Jiang L, Erb H, Johnson JA, Murphy TH (2003). Coordinate regulation of glutathione biosynthesis and release by Nrf2-expressing glia potentially protects neurons from oxidative stress. *J Neurosci* **23**: 3394–3406.
- Shikova E, Lin YC, Saha K, Brooks BR, Wong PKY (1993). Correlation of specific virus-astrocyte interactions and cytopathic effects induced by ts1, a neurovirulent mutant of Moloney murine leukemia virus. *J Virol* **67**: 1137–1147.
- Siklos L, Engelhardt JI, Reaume AG, Scott RW, Adalbert R, Obal I, Appel SH (2000). Altered calcium homeostasis in spinal motoneurons but not in oculomotor neurons of SOD-1 knockout mice. *Acta Neuropathol (Berl)* **99**: 517–524.
- Stoica G, Illanes O, Tasca SI, Wong PKY (1993). Temporal central and peripheral nervous system changes induced by a paralytogenic mutant of Moloney murine leukemia virus TB. *Lab Invest* **69**: 724–735.
- Stoica G, Tasca SI, Wong PKY (2000). Motor neuronal loss and neurofilament-ubiquitin alteration in MoMuLV-ts1 encephalopathy. *Acta Neuropathol (Berl)* **99**: 238–244.
- Su HL, Liao CL, Lin YL (2002). Japanese encephalitis virus infection initiates endoplasmic reticulum stress and an unfolded protein response. *J Virol* **76**: 4162–4171.
- Szurek PF, Yuen PH, Ball JK, Wong PKY (1990). A Val-25-to-Ile substitution in the envelope precursor polypeptide, gPr80env, is responsible for the temperature sensitivity, inefficient processing of gPr80env, and neurovirulence of ts1, a mutant of Moloney murine leukemia virus TB. *J Virol* **64**: 467–475.
- Urano F, Wang X, Bertolotti A, Zhang Y, Chung P, Harding HP, Ron D (2000). Coupling of stress in the ER to activation of JNK protein kinases by transmembrane protein kinase IRE1. *Science* **287**: 664–666.
- Waris G, Tardif KD, Siddiqui A (2002). Endoplasmic reticulum (ER) stress hepatitis C virus induces an ER-nucleus signal transduction pathway and activates NF-kappaB and STAT-3. *Biochem Pharmacol* **64**: 1425–1430.
- Wong PKY, Lynn WS (1997). Neuroimmunodegeneration. *EOS J Immunol Immunopharmacol* **17**: 30–35.
- Wong PKY, Lynn WS, Lin YC, Choe W, Yuen PH (1998). ts1 MoMuLV: A murine model of neuroimmunodegeneration. In: *Neuroimmunodegeneration*. Wong PKY, Lynn WS (eds). Heidelberg: R.G. Landes, pp 75–93.
- Yoshida H, Matsui T, Yamamoto A, Okada T, Mori K (2001). XBP1 mRNA is induced by ATF6 and spliced by IRE1 in response to ER stress to produce a highly active transcription factor. *Cell* **107**: 881–891.
- Yoshida H, Okada T, Haze K, Yanagi H, Yura T, Negishi M, Mori K (2000). ATF6 activated by proteolysis binds in the presence of NF-Y (CBF) directly to the cis-acting element responsible for the mammalian unfolded protein response. *Mol Cell Biol* **20**: 6755–6767.